Towards high charge-carrier mobilities by rational design of the shape and periphery of discotics

Xinliang Feng[1], Valentina Marcon[1], Wojciech Pisula[1]*, Michael Ryan Hansen[1], James Kirkpatrick[2], Ferdinand Grozema[3], Denis Andrienko[1†], Kurt Kremer[1] and Klaus Müllen[1†]

Discotic liquid crystals are a promising class of materials for molecular electronics thanks to their self-organization and charge transporting properties. The best discotics so far are built around the coronene unit and possess six-fold symmetry. In the discotic phase six-fold-symmetric molecules stack with an average twist of 30°, whereas the angle that would lead to the greatest electronic coupling is 60°. Here, a molecule with three-fold symmetry and alternating hydrophilic/hydrophobic side chains is synthesized and X-ray scattering is used to prove the formation of the desired helical microstructure. Time-resolved microwave-conductivity measurements show that the material has indeed a very high mobility, $0.2\,cm^2\,V^{-1}\,s^{-1}$. The assemblies of molecules are simulated using molecular dynamics, confirming the model deduced from X-ray scattering. The simulated structures, together with quantum-chemical techniques, prove that mobility is still limited by structural defects and that a defect-free assembly could lead to mobilities in excess of $10\,cm^2\,V^{-1}\,s^{-1}$.

D iscotic thermotropic liquid crystals combine unique material properties, such as fluidity and the inability to support shear stress, with anisotropic mechanical and optical properties[1–4]. This combination is a consequence of the molecular self-organization into columnar structures, where the molecules stack on top of one another into columns, which then arrange in a regular lattice. The anisotropy of macroscopic properties arises from the anisotropy of the molecules, in our case flat aromatic cores with aliphatic chains attached at the edges, and the global orientational ordering of molecules.

The most striking property of discotics, however, is their ability to conduct charges along the stacks of aromatic cores, which can be used in various organic devices, such as field-effect transistors[5,6] and photovoltaic cells[7]. To guarantee efficient operation, high charge-carrier mobilities along the columns are required[8,9]. To achieve high mobilities, two distinct but related problems must be addressed: first, compounds must have good self-organizing abilities, ensuring defect-free mesophases on a large spatial scale. Second, the local molecular arrangement in these mesophases has to be optimal for the charge transport. Hence, to rationally design these compounds, we have to (1) identify the best local molecular arrangement of all (synthesizable) aromatic cores and (2) manipulate the periphery (side chains) to achieve this arrangement and at the same time to obtain good self-organizing abilities.

We will first discuss the optimal choice of local molecular arrangements. Charge transport in discotic liquid crystals can be described using a thermally activated hopping formalism with the rate of hops given by semiclassical non-adiabatic high-temperature Marcus theory. The higher this rate is, the faster an electron (hole) moves along the column, and the higher the corresponding mobility is. According to Marcus theory the rate of charge transfer between two identical molecules ω depends on
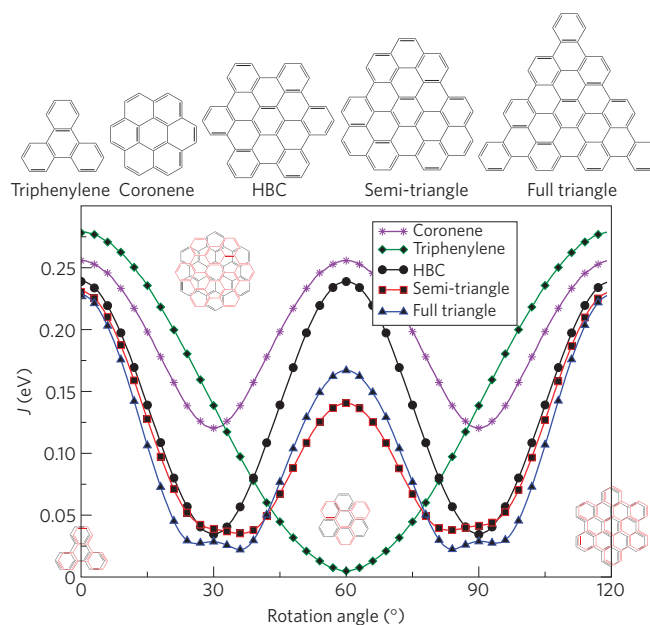

Figure 1 | Absolute value of the transfer integral J as a function of the azimuthal rotation angle for several symmetric polyaromatic hydrocarbon cores. The separation was fixed to 0.36 nm. The insets illustrate face-to-face and staggered stacking of two typical disc-shaped molecules: triphenylene (staggered twisting angle is 60°) and HBC (staggered twisting angle is 30°). Note that even though the maxima of the overlap integral decrease with the increase of the core size, the overall hopping rate ω increases owing to the simultaneous decrease of the reorganization energy λ.

[1]Max Planck Institute for Polymer Research, Ackermannweg 10, 55128 Mainz, Germany, [2]Department of Physics, Imperial College London, Prince Consort Road, London SW7 2BW, UK, [3]DelftChemTech, Delft University of Technology, Julianalaan 136, 2628 BL Delft, The Netherlands. *Present address: Evonik Degussa GmbH, Process Technology & Engineering, Process Technology - New Processes, Rodenbacher Chaussee 4, 63457 Hanau-Wolfgang, Germany. [†]e-mail: denis.andrienko@mpip-mainz.mpg.de; muellen@mpip-mainz.mpg.de.
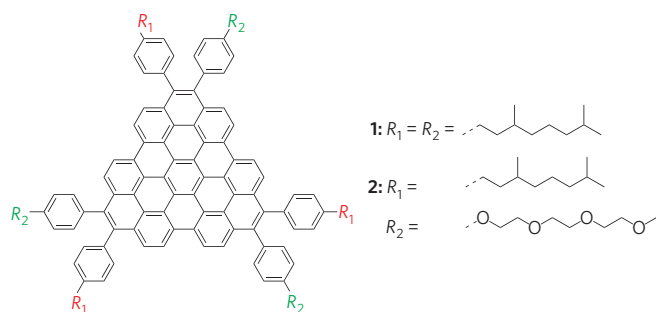
Figure 2 | Structures of the compounds studied.

two key parameters: the reorganization energy λ and the transfer integral J (refs 10, 11):

$$\omega = \frac{J^2}{\hbar}\sqrt{\frac{\pi}{\lambda k_B T}} \exp\left[-\frac{\lambda}{4 k_B T}\right]$$

where $\hbar$ is Planck's constant, k_B Boltzmann's constant and T the temperature.

The reorganization energy λ is strongly related to the self-trapping energy of a charge and decreases with increasingly large conjugated cores; for example, for triphenylene it is 0.18 eV, for coronene 0.13 eV and for hexa-peri-hexabenzocoronene (HBC) 0.1 eV. Hence, larger conjugated cores favour higher hopping rates and hence higher charge-carrier mobilities[12]. The reorganization energy is not sensitive to the relative positions/orientations of neighbouring molecules[13,14].

The transfer integral J describes the probability of electron tunnelling between two neighbouring molecules. As it is intimately related to molecular overlap, it is very sensitive to relative positions and orientations of neighbours. J decays exponentially as a function of the intermolecular separation z (for example for HBC, shown in Fig. 1, this dependence is $J \sim \exp(-2.2z/\text{Å})$). Hence, compounds with smaller intermolecular distance should have higher charge mobility. On the other hand, the transfer integral is very sensitive to the lateral orientation and rotational registration of neighbours. Analysing these dependencies for a set of symmetric cores, shown in Fig. 1, we can conclude that the most favourable molecular arrangement for the charge transport is either co-facial (0° twist)

or twisted by 60° (except triphenylene). The value of the transfer integral decreases very rapidly with the angle; for example, for a 10° twist the value is already about half that for 0°. Hence, for efficient charge transport it is preferable to lock the relative molecular orientations at the positions of the maxima of the transfer integral.

Summarizing the predictions of the Marcus theory, we can narrow down the tasks of the side chains: apart from providing processability and good self-assembling properties they should (1) favour small intermolecular separations and (2) provide either a cofacial or a 60° twist molecular arrangement. The cofacial arrangement often leads to steric repulsions of the side chains, larger intermolecular separations and widening of the statistical distribution of transfer integrals, which is known to decrease the charge mobility[15,16]. Naturally, compounds with six-fold symmetry (for example hexaalkyl-substituted HBC) are in a face-to-face arrangement for both 0° and 60° twists between the neighbours and have the same drawbacks. From this simple microscopic prediction, our conclusion is that, among the considered compounds, molecules of three-fold symmetry (for example, triangularly shaped polyaromatic hydrocarbons, Fig. 1) with a helical packing structure and 60° twist should provide optimal local arrangement for the charge transport.

To achieve such a helical molecular packing, we can borrow examples from nature, where the helical organization can be found in the double helices formed by DNA and the α-helical motifs in proteins[17–19]. Nature exploits a great variety of interactions to control this self-organization, from steric repulsion, hydrogen bonding, van der Waals forces and π–π stacking to electrostatic interactions[17,20,21]. A minor change in the molecular architecture may dramatically influence the subtle balance of non-covalent interactions between molecules[22]. In the case of polyaromatic hydrocarbons, we can vary the size and the shape of the conjugated core as well as the type of attached side chain[9,23]. By tuning these 'molecular parameters', compounds with different abilities to self-organize and conduct charge carriers can be obtained[9,24,25].

Semi-triangle-shaped molecules **1** (with six achiral 3,7-dimethyloctylphenyl substituents, Fig. 2) have previously been reported to show highly ordered helical superstructures including three molecules in one helical pitch[26], corresponding to a twist angle of 40°. In this work, using alternating hydrophilic/hydrophobic side chains (**2**, with three pairs of alternating alkylphenyl and triethyleneglycolphenyl substituents, Fig. 2) we demonstrate that
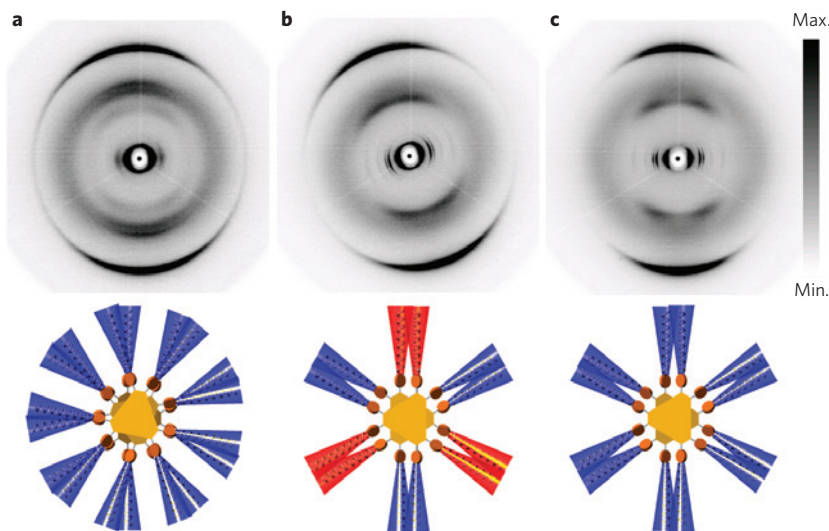

Figure 3 | Two-dimensional wide-angle X-ray scattering patterns and corresponding schematic illustrations of top-viewed molecules stacked on top of one another. a, Compound **1**; **b**, compound **2**; both patterns recorded at 30 °C; **c**, compound **1** at 180 °C. Blue and red substituents indicate alkyl and glycol chains respectively.
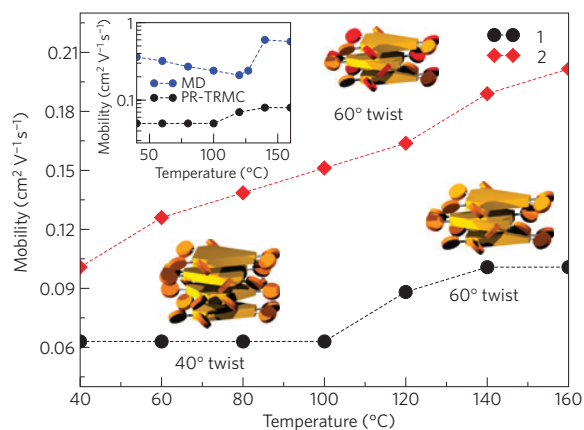
Figure 4 | Charge mobilities as a function of temperature as measured by the PR-TRMC technique. The inset shows the direct comparison with simulations for **1**.

it is possible to achieve staggered stacking of large graphene-like discotics within columnar assemblies, with a twist angle of 60°. This novel assembly is due to complementary hydrophobic–hydrophilic and π–π interactions. We use a two-pronged method to assess the changes in morphology due to changes in the type of side chain: X-ray scattering provides information about changes in global ordering of the columns, whereas the measurement (by pulse-radiolysis time-resolved microwave conductivity, PR-TRMC) and simulation (by the method outlined in refs 16, 27) of local one-dimensional charge mobility give information about the quality of the ordering of the columns. We achieve a twist angle of 60° for either **2** with glycol side chains, or for a high-temperature phase of **1** with only alkyl side chains. PR-TRMC measurements show that those phases with a 60° twist indeed have a higher mobility. The simulations show that the mobilities obtained are consistent with morphologies that accommodate a rather large amount of structural disorder. We therefore make the prediction that better processing will lead to higher charge mobilities.

The synthesis of molecule **2** is shown in Supplementary Information. Characterizations by nuclear magnetic resonance (NMR) spectroscopy, elemental analysis and matrix-assisted laser desorption/ionization–time of flight mass spectroscopy are shown to be in full agreement with the structure presented.

Differential scanning calorimetry did not show any phase transition for **1** and **2** over the temperature range between −150 and 250 °C. Two-dimensional wide-angle X-ray scattering experiments on mechanically aligned filaments were carried out to gain an insight into the influence of the different substitution patterns on supramolecular organization of both compounds. The two-dimensional patterns at 30 °C in Fig. 3a,b indicate in both cases well-oriented hexagonal columnar structures characterized by equatorial reflections at relative reciprocal spacing of $1:\sqrt{3}:2$, typical for liquid crystalline phases of discotic systems. The derived unit-cell parameters are $a_{hex} = 3.41$ nm for **1** and $a_{hex} = 3.19$ nm for **2**. The disc-shaped molecules are arranged in the stacks with their molecular planes perpendicular to the columnar axis. The intracolumnar π-stacking distance of 0.36 nm for **1** and **2** is represented by the sharp wide-angle meridional reflections. Furthermore, the appearance of additional meridional reflections in the middle-angle scattering range of both patterns suggests more complex superstructures. In the case of **1**, the first (off-)meridional reflections on the hkl layer line at a related spacing of 1.1 nm (Fig. 3a) indicate an identical lateral order of every fourth molecule along the stacking direction (for detailed analysis see Supplementary Information). The appearance of such layer lines of scattering intensities is typical for a helical
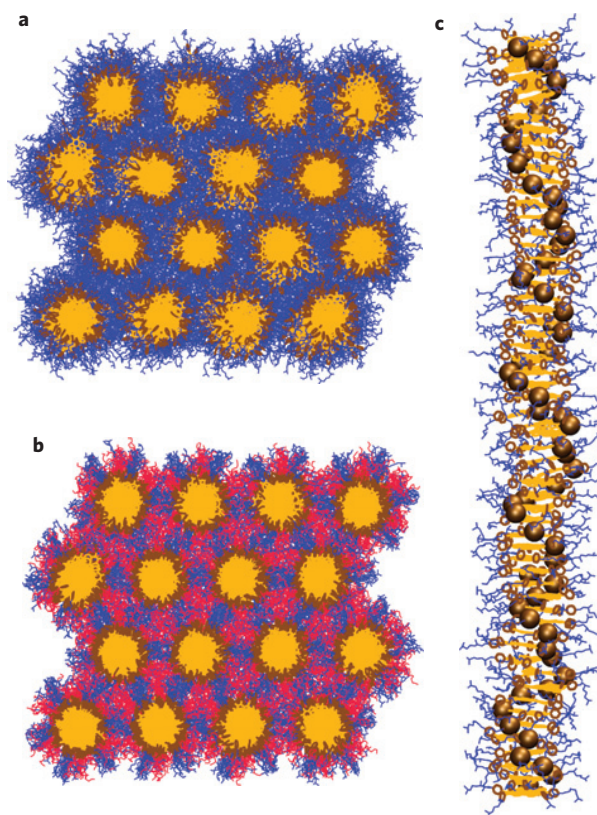

Figure 5 | Representative simulation snapshots. a, Compound **1**, with 40° twist angle; **b**, compound **2**, with 60° twist. Glycol side chains are shown in red. The side chains of the same nature segregate owing to hydrophobic/hydrophilic interactions helping the staggered packing of **2**. **c**, Side view of a single column. The blobs illustrate helical molecular packing.

molecular arrangement, and has also been observed in other discotic molecules[13,28–31], DNA mesophases[32,33], dendrimers[17,34], macrocycles[35] and polymers[36,37]. In addition, our work on liquid crystalline HBCs proved that the adopted analysis of two-dimensional patterns agrees with theoretical predictions of helical intracolumnar packing[38,39]. Therefore, neighbouring molecules of **1** in the column are successively rotated laterally by 40° towards one another, leading to a helical stacking with three molecules per pitch[23,26]. Figure 3a presents a schematic illustration of a top-viewed stack with three molecules of **1**. In contrast, the two-dimensional pattern of compound **2** showed only one middle-angle reflection, corresponding to a distance of 0.72 nm, which is twice the value of a simple π-stacking distance (Fig. 3b). The molecules of **2** rotate by 60°, leading to a staggered packing with every second disc in an identical position. The schematic illustration in Fig. 3b shows that the substituents of the same character of neighbouring discs fall together at this rotational angle. The smaller rotational angle for **1** (as compared to **2**) results in a denser alkyl mantle around the aromatic stack and thus in a larger hexagonal unit cell. Both compounds have been assigned to the plastic crystalline phase over the whole temperature range[40]. This phase differs from the typical crystalline and disordered liquid crystalline phases of discotics.

Considering the similar molecular structures and substitution pattern, the difference in intracolumnar packing between **1** and **2** is clearly due to hydrophobic/hydrophilic interactions of the side chains in the disc periphery. What is even more fascinating is that the X-ray pattern of **1** recorded at 180 °C also shows a staggered packing (no phase transition was detected by differential scanning calorimetry), indicating that the bulky phenyl substituents and entropic contribution of alkyl side chains are also important. The
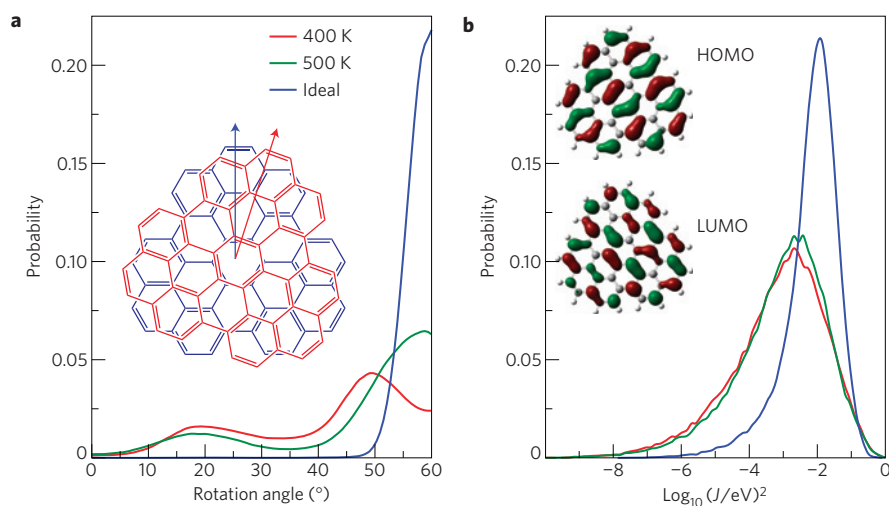
Figure 6 | Distribution functions of the relative molecular orientations and transfer integrals. a, Distribution functions of the relative orientations between the nearest neighbours for **1** using different equilibration procedures. The inset illustrates the definition of the rotation angle. **b**, Corresponding distribution functions of the transfer integrals. The inset shows the highest occupied molecular orbital (HOMO) and lowest unoccupied molecular orbital (LUMO) used for the evaluation of transfer integrals.

transition to the staggered packing of **1** at high temperatures can be attributed to the increased steric hindrance of the attached phenyl groups and alkyl side chains. On heating, the flexible alkylphenyl chains acquire larger excluded volume, which forces the stacked discs of **1** to rotate with respect to one another, reaching the twisting angle of 60°. The change in the pitch is reversible: cooling the sample back to 30 °C recovers the helical arrangement of **1** with the molecular rotation of 40°.

The solid-state NMR experiments[41] also show different two-dimensional line shapes of the inner core protons for the two compounds. These differences originate from the different local $\pi-\pi$ packing of **1** and **2**, with more pronounced features for **2**, which could imply a more ordered intracolumnar molecular packing, in agreement with the proposed structures. Further details and interpretations of the solid-state NMR results are given in Supplementary Information.

Charge dynamics has been assessed using PR-TRMC measurements of the temperature dependence of mobility[42], which is shown in Fig. 4. PR-TRMC, in contrast to the time of flight measurements, senses only the local molecular ordering, and provides the mobility of small well-ordered domains of the material.

As can be seen from Fig. 4, the absolute mobility values of the plastic crystalline **1** and **2** are of the same order as the mobility of HBC with linear alkyl chains in a crystalline phase (0.18 cm² V⁻¹ s⁻¹ when measured using the same protocol). This is rather surprising, because typically crystalline, and thus more ordered, systems possess much higher mobilities in comparison with non-crystalline materials. The mobility of **1** is practically temperature independent until 120 °C but then sharply increases by about 30%. This is in agreement with our earlier observations of higher charge transfer rates at 60° twist (due to higher overlap integrals) and structural transition resulting in better helical winding at high temperatures. In contrast, the mobility of **2** increases monotonically with temperature, which is typical for discotics[43].

To further relate the mobility changes to the microscopic molecular arrangement, we have carried out molecular-dynamics simulations and charge-mobility calculations for columnar arrangements of **1** and **2**. For each system, 960 molecules were arranged in columns of 60 molecules each, with hexagonal arrangement of the columns. Within the columns, the molecules were aligned in a helical fashion, with initial twist angle of 40° between the neighbouring molecules. Simulation details, as well as the methods

used for evaluation of transfer integrals, reorganization energies and charge dynamics, are given in Supplementary Information.

After equilibration we observe that the molecules are well ordered within the columns, with their molecular planes oriented perpendicular to the columnar axes. Small undulations of the columns are also observed, which are due to thermal fluctuations of the molecular director. Representative snapshots of the systems are shown in Fig. 5.

Molecular dynamics predicts lattice constants of about 2.93 nm for **1**, and 2.94 nm for **2**. Both values of the simulated lattice constants are smaller than those provided by X-ray scattering, suggesting that the molecules in our simulations are somewhat more tightly packed and ordered. To characterize the helical order, we calculated the distributions of the twist angle between the nearest neighbours (defined as a probability of finding two neighbours rotated with respect to each other at an angle φ), which are shown in Fig. 6a. Here, three distributions are shown for **1**. The first one had an initial helicity of 40° and was equilibrated at 400 K. The second one was annealed at 500 K, starting from the final configuration obtained from the equilibration at 400 K. Finally, the last one corresponds to an 'ideal' situation, where we prepared well-ordered system with 60° twist and then annealed it at 500 K.

For **1**, the average twist angle (which is defined as an average of the lateral rotation angle between molecules i and $i+1$) does not change during equilibration, and is around 40°. However, the helix has a 'secondary' structure, with two maxima, around 20° and 50°. On heating to 500 K the average value shifts to 60°, similar to the experimentally observed transition in a helical pitch. On the other hand, the distribution for molecules **2** always has a maximum at 60°.

Furthermore, to check the value of the pitch of the helical structure, several initial configurations with different twist angles and consequently different helical pitches were prepared for both lattices. After annealing at 450 K they all converged to the structure with the average twist angle of 60° (see Supplementary Information), indicating that the system with 60° twist is an equilibrium one. This also disentangles molecular dynamics and X-ray predictions, and hence confirms the helical molecular arrangement deduced from the X-ray data.

To relate particular molecular ordering to charge mobility, we first consider the distributions of the transfer integrals, shown in Fig. 6b, which account for both lateral and out-of-plane molecular fluctuations. As we are dealing with one-dimensional transport, the

value of the mobility is limited by the tail of the small transfer integrals; that is, the width of the distribution is important: the sharper the peak is, the higher the mobility is (provided the position of the peak does not change)[13,44].

What simulations show is that the distributions for 400 K and 500 K are very similar: the only difference is a slight shift of the maximum towards higher values at 500 K with a slightly lower tail of small transfer integrals. This of course increases the value of the mobility: the calculated value for **1** is 0.24 cm^2 V^{-1} s^{-1} at 400 K, which increases to 0.42 cm^2 V^{-1} s^{-1} at 500 K. The calculated mobility of **2** at 400 K was 0.58 cm^2 V^{-1} s^{-1}. The calculated numbers differ by a factor of two from the experimentally measured values; however, the ratios between the mobilities for **2** and **1** and high/low-temperature mesophase of **1** are in excellent agreement. Possible sources of overestimation, such as energetic disorder due to the electrostatic and polarization contributions, which are being ignored here, as well as the external reorganization energy, are discussed in detail in refs 45 and 46. Including additional sources of disorder, as well as leading to smaller mobilities, would also lead to less negatively dependent temperature dependence of charge mobility.

It is known that appropriate processing can significantly improve the value of the mobility (for example, thermal annealing can increase its value by an order of magnitude)[22,42]. Therefore, it is important to know the upper limit for the mobility in the 'ideal' system, where we include all local fluctuations but exclude structural defects. Here simulations are extremely powerful, because we can prepare a desirable molecular arrangement and locally equilibrate the system. Our simulations suggest that, even though on annealing the average pitch of the helices becomes closer to the ideal 60°, it is not perfect. The presence of a structural defect (the peaks at ∼20°) results in a drastic (two orders of magnitude) reduction of the charge mobility. Indeed, for the system with the prearranged 60° twist, the molecular distribution is significantly sharper than that for the one with the initial twist of 40°, even after annealing at 500 K, owing to efficient locking of the rotational molecular motion by the bulky phenyl groups. Correspondingly, the distribution of the transfer integrals has a sharp peak with a small tail of small overlap integrals, which, within the Marcus picture of hopping transport, gives the mobility value of 15.9 cm^2 V^{-1} s^{-1}. Hence, the prime task for material scientists is to engineer processing methods able to suppress these structural defects.

In conclusion, using Marcus theory to calculate the parameters of temperature-activated charge transfer, we have outlined the criteria for the rational design of polyaromatic hydrocarbons with high charge-carrier mobilities. Our prediction is that the triangularly shaped compounds with a large core, stacked on top of one another in a staggered fashion, with 60° twist between neighbours, should possess high charge-carrier mobility, paving the way for the broad application of discotic semiconductor materials in the future.

References

1. Demus, D., Goodby, J., Gray, G. W., Spiess, H. W. & Vill, V. *Handbook of Liquid Crystals* (Wiley–VCH, 1998).
2. Laschat, S. *et al.* Discotic liquid crystals: From tailor-made synthesis to plastic electronics. *Angew. Chem. Int. Ed.* **46**, 4832–4887 (2007).
3. Sergeyev, S., Pisula, W. & Geerts, Y. H. Discotic liquid crystals: A new generation of organic semiconductors. *Chem. Soc. Rev.* **36**, 1902–1929 (2007).
4. van de Graats, A. M. *et al.* The mobility of charge carriers in all four phases of the columnar discotic material hexakis(hexylthio)triphenylene: Combined TOF and PR-TRMC results. *Adv. Mater.* **8**, 823–826 (1996).
5. Xiao, S. X. *et al.* Molecular wires from contorted aromatic compounds. *Angew. Chem. Int. Ed.* **44**, 7390–7394 (2005).
6. Pisula, W. *et al.* A zone-casting technique for device fabrication of field-effect transistors based on discotic hexa-peri-hexabenzoeoronene. *Adv. Mater.* **17**, 684–689 (2005).
7. Schmidt-Mende, L. *et al.* Self-organized discotic liquid crystals for high-efficiency organic photovoltaics. *Science* **293**, 1119–1122 (2001).
8. van de Craats, A. M. *et al.* Record charge carrier mobility in a room-temperature discotic liquid-crystalline derivative of hexabenzocoronene. *Adv. Mater.* **11**, 1469–1472 (1999).
9. Adam, D. *et al.* Fast photoconduction in the highly ordered columnar phase of a discotic liquid-crystal. *Nature* **371**, 141–143 (1994).
10. Marcus, R. A. Electron-transfer reactions in chemistry—theory and experiment. *Rev. Mod. Phys.* **65**, 599–610 (1993).
11. Freed, K. F. & Jortner, J. Multiphonon processes in nonradiative decay of large molecules. *J. Chem. Phys.* **52**, 6272–6291 (1970).
12. Coropceanu, V. *et al.* Charge transport in organic semiconductors. *Chem. Rev.* **107**, 926–952 (2007).
13. Lemaur, V. *et al.* Charge transport properties in discotic liquid crystals: A quantum-chemical insight into structure–property relationships. *J. Am. Chem. Soc.* **126**, 3271–3279 (2004).
14. Cornil, J., Lemaur, V., Calbert, J. P. & Bredas, J. L. Charge transport in discotic liquid crystals: A molecular scale description. *Adv. Mater.* **14**, 726–729 (2002).
15. Bassler, H. Charge transport in disordered organic photoconductors—a Monte-Carlo simulation study. *Phys. Status Solidi B* **175**, 15–56 (1993).
16. Kirkpatrick, J., Marcon, V., Nelson, J., Kremer, K. & Andrienko, D. Charge mobility of discotic mesophases: A multiscale quantum and classical study. *Phys. Rev. Lett.* **98**, 227402 (2007).
17. Percec, V., Won, B. C., Peterca, M. & Heiney, P. A. Expanding the structural diversity of self-assembling dendrons and supramolecular dendrimers via complex building blocks. *J. Am. Chem. Soc.* **129**, 11265–11278 (2007).
18. Prins, L. J., Huskens, J., de Jong, F., Timmerman, P. & Reinhoudt, D. N. Complete asymmetric induction of supramolecular chirality in a hydrogen-bonded assembly. *Nature* **398**, 498–502 (1999).
19. Papapostolou, D. *et al.* Engineering nanoscale order into a designed protein fiber. *Proc. Natl Acad. Sci. USA* **104**, 10853–10858 (2007).
20. Shimizu, T., Masuda, M. & Minamikawa, H. Supramolecular nanotube architectures based on amphiphilic molecules. *Chem. Rev.* **105**, 1401–1443 (2005).
21. Hoeben, F. J. M., Jonkheijm, P., Meijer, E. W. & Schenning, A. About supramolecular assemblies of pi-conjugated systems. *Chem. Rev.* **105**, 1491–1546 (2005).
22. McCulloch, I. *et al.* Liquid-crystalline semiconducting polymers with high charge-carrier mobility. *Nature Mater.* **5**, 328–333 (2006).
23. Feng, X., Pisula, W. & Mullen, K. From helical to staggered stacking of zigzag nanographenes. *J. Am. Chem. Soc.* **129**, 14116–14117 (2007).
24. Pisula, W. *et al.* Relation between supramolecular order and charge carrier mobility of branched alkyl hexa-peri-hexabenzocoronenes. *Chem. Mater.* **18**, 3634–3640 (2006).
25. Kastler, M. *et al.* Organization of charge-carrier pathways for organic electronics. *Adv. Mater.* **18**, 2255–2259 (2006).
26. Feng, X. L. *et al.* Triangle-shaped polycyclic aromatic hydrocarbons. *Angew. Chem. Int. Ed.* **46**, 3033–3036 (2007).
27. Andrienko, D., Kirkpatrick, J., Marcon, V., Nelson, J. & Kremer, K. Structure–charge mobility relation for hexabenzocoronene derivatives. *Phys. Status Solidi B* **245**, 830–834 (2008).
28. Holst, H. C., Pakula, T. & Meier, H. Liquid crystals in the series of 2,4,6-tristyryl-1,3,5-triazines. *Tetrahedron* **60**, 6765–6775 (2004).
29. Barbera, J. *et al.* Supramolecular helical stacking of metallomesogens derived from enantiopure and racemic polycatenar oxazolines. *J. Am. Chem. Soc.* **125**, 4527–4533 (2003).
30. Gearba, R. I. *et al.* Mesomorphism, polymorphism, and semicrystalline morphology of poly(di-n-propylsiloxane). *Macromolecules* **39**, 988–999 (2006).
31. Barbera, J. *et al.* Cyclotriphosphazene as a dendritic core for the preparation of columnar supermolecular liquid crystals. *Chem. Mater.* **18**, 5437–5445 (2006).
32. Livolant, F., Levelut, A. M., Doucet, J. & Benoit, J. P. The highly concentrated liquid-crystalline phase of DNA is columnar hexagonal. *Nature* **339**, 724–726 (1989).
33. Watson, J. D. & Crick, F. H. C. Molecular structure of nucleic acids—a structure for deoxyribose nucleic acid. *Nature* **171**, 737–738 (1953).
34. Percec, V. *et al.* Self-assembly of semifluorinated minidendrons attached to electron-acceptor groups into pyramidal columns. *Chem. Eur. J.* **13**, 3330–3345 (2007).
35. Pisula, W., Kastler, M., Yang, C., Enkelmann, V. & Mullen, K. Columnar mesophase formation of cyclohexa-m-phenylene-based macrocycles. *Chem. Asian J.* **2**, 51–56 (2007).
36. Percec, V. *et al.* Synthesis, structural, and retrostructural analysis of helical dendronized poly(1-naphthylacetylene)s. *J. Polym. Sci. A* **45**, 4974–4987 (2007).
37. Sakurai, S. I. *et al.* Two-dimensional helix-bundle formation of a dynamic helical poly(phenylacetylene) with achiral pendant groups on graphite. *Angew. Chem. Int. Ed.* **46**, 7605–7608 (2007).

38. Pisula, W. *et al.* Helical packing of discotic hexaphenyl hexa-peri-hexabenzocoronenes: Theory and experiment. *J. Phys. Chem. B* **111**, 7481–7487 (2007).

39. Wu, J. S., Watson, M. D., Zhang, L., Wang, Z. H. & Mullen, K. Hexakis(4-iodophenyl)-peri-hexabenzocoronene—A versatile building block for highly ordered discotic liquid crystalline materials. *J. Am. Chem. Soc.* **126**, 177–186 (2004).

40. Glusen, B., Heitz, W., Kettner, A. & Wendorff, J. H. A plastic columnar discotic phase D-p. *Liquid Cryst.* **20**, 627–633 (1996).

41. Brown, S. P. & Spiess, H. W. Advanced solid-state NMR methods for the elucidation of structure and dynamics of molecular, macromolecular, and supramolecular systems. *Chem. Rev.* **101**, 4125–4155 (2001).

42. van de Graats, A. M. *et al.* The mobility of charge carriers in all four phases of the columnar discotic material hexakis(hexylthio)triphenylene: Combined TOF and PR-TRMC results. *Adv. Mater.* **8**, 823–826 (1996).

43. Debije, M. G. *et al.* The optical and charge transport properties of discotic materials with large aromatic hydrocarbon cores. *J. Am. Chem. Soc.* **126**, 4641–4645 (2004).

44. Deng, W. Q. & Goddard, W. A. Predictions of hole mobilities in oligoacene organic semiconductors from quantum mechanical calculations. *J. Phys. Chem. B* **108**, 8614–8621 (2004).

45. Marcon, V. *et al.* Columnar mesophases of hexabenzocoronene derivatives. I. Phase transitions. *J. Chem. Phys.* **129**, 094505 (2008).

46. Kirkpatrick, J., Marcon, V., Kremer, K., Nelson, J. & Andrienko, D. Columnar mesophases of hexabenzocoronene derivatives: II. Charge carrier mobility. *J. Chem. Phys.* **129**, 094506 (2008).

Additional information

Supplementary information accompanies this paper on www.nature.com/naturematerials. Reprints and permissions information is available online at http://npg.nature.com/reprintsandpermissions. Correspondence and requests for materials should be addressed to D.A. or K.M.